Near-surface soil moisture estimation by combining airborne L-band brightness temperature observations and imaging hyperspectral data at the field scale

Marion Pause,[a,c] Karsten Schulz,[b] Steffen Zacharias,[c] and Angela Lausch[d]
[a]University of Tuebingen, WESS—Water & Earth System Science Competence Centre, Hölderlinstraße 12, 72074 Tübingen, Germany
marion.pause@uni-tuebingen.de
[b]Ludwig-Maximilians-Universität München, Department of Geography, Luisenstr. 37, 80333 München, Germany
[c]Helmholtz-Centre for Environmental Research—UFZ, Department Monitoring and Exploration Technologies, Permoserstr. 15, 04318 Leipzig, Germany
[d]Helmholtz-Centre for Environmental Research—UFZ, Department Computational Landscape Ecology, Permoserstr. 15, 04318 Leipzig, Germany

Abstract. The observation of spatially distributed soil moisture fields is an essential component for a large range of hydrological, climate, and agricultural applications. While direct measurements are expensive and limited to small spatial domains, the inversion of airborne and satellite L-band radiometer data has shown the potential to provide spatial estimates of near surface soil moisture from the local up to the global scale. When using L-band radiometer observations for soil moisture retrieval, a major limitation is the attenuation of the microwave signal by the vegetation, hampering the signal inversion and thereby making spatially distributed plant information necessary. Usually vegetation types are considered with a vegetation type specific global parameterization, e.g., for leaf area index (LAI). Within this study we evaluate and address the effect of spatially varying LAI on high spatial resolution (pixel size 50 m) airborne L-band brightness temperature of crop canopies that are usually regarded homogeneous. To account for within field variations of LAI we used airborne imaging spectrometer data (pixel size 1.5 m) to empirically create maps of LAI using spectral greenness vegetation indices. We found clear ($R^2 < 0.90$) functional relationships between spatially varying L-band brightness temperature and LAI variations within crop canopies that in literature are usually assumed homogeneous. Very good ($R^2 = 0.93$) near surface soil moisture estimates were achieved using multi-variate regression and adding plant specific spectral information to the independent variable set for final soil moisture retrieval. The study shows that a multi-sensor campaign using airborne L-band radiometer and imaging spectrometers provide a powerful data set for monitoring patterns of near surface soil moisture and vegetation canopy at the field scale with high accuracy. [DOI: 10.1117/1.JRS.6.063516]

Keywords: near surface soil moisture; L-band brightness temperature; leaf area index; regression models.

Paper 11226 received Oct. 20, 2011; revised manuscript received Jan. 27, 2012; accepted for publication Feb. 27, 2012; published online Apr. 27, 2012.

1 Introduction

Near surface soil moisture is one of the dominant controls for a large variety of environmental processes including, e.g., the partitioning of water and energy fluxes at the land surface into rainfall, surface runoff, infiltration, and evapotranspiration. It plays a major role for biogeochemical processes of driving global matter fluxes, or the redirection of incoming solar radiation into albedo, thermal radiation, and sensible and latent heat fluxes. Also, the temporal dynamics of soil moisture patterns are well known to be related to integral system (catchment) responses and

0091-3286/2012/$25.00 © 2012 SPIE

states at different spatial scales including threshold-like behavior,[1–3] and therefore require precise detection and monitoring.

In general, a large number of soil moisture measurement methods applied to different spatial scales exists that can be broadly defined into two main methods[4]: Contact-based methods require direct contact with the soil and include capacitance sensors, time domain reflectometry, electrical resistivity measurements, heat pulse sensors, fiber optic sensors, and destructive sampling (e.g., gravimetric methods) and are usually limited to the point scale. However they are currently extended to so-called wireless sensor networks to derive spatial soil moisture information with high temporal resolution at the hillslope and small catchment scale.[5] An excellent review of these methods is provided, e.g., by Ref. 6.

The second category consists of contact-free measurement techniques and here, remote sensing and hydro-geophysical methods are most prominent. Hydro-geophysical methods include off-ground penetrating radar and electromagnetic induction and, although suited for campaign based mapping, they are too expensive for providing high temporal resolution soil moisture data at the catchment scale.[4] Remote sensing methods include passive microwave radiometers, synthetic aperture scatterometers, and thermal methods that are operated either ground based, or from airborne or spaceborne platforms[7,8] and are able to provide spatial distributed soil moisture information over large areas. In particular, the inversion of microwave radiometer data has recently shown increasing potential to provide spatial estimates of near surface soil moisture and is subject of investigation here.

The retrieval of surface soil moisture from L-band radiometers (frequency $f = 1$ to 2 GHz, wavelength $\lambda = 30$ to 15 cm) from aircraft and satellite platforms received a significant upturn during the last 10 years.[7–9] Particularly, the European Space Agency's (ESA) soil moisture and ocean salinity (SMOS) mission initialized a high number of spatial high resolution airborne L-band radiometer campaigns to analyze scale dependent soil moisture sensitivities.[10,11]

The availability of high spatial resolution airborne L-band radiometer data provides a data product that is applicable for monitoring of near surface soil moisture at the field scale as required for agricultural applications. Since the detection of microwave emission at L-band from an aircraft is almost weather independent, high temporal monitoring is possible. L-band brightness temperature (TB) data offers a nearly linear relationship to surface soil moisture, given uniform vegetation and soil characteristics.[12]

Vegetation absorbs and scatters microwave radiation from the soil and contributes its own emission to the signal received. Therefore it is essential to provide information about the vegetation covering the soil. Usually there are vegetation-type specific parameterizations (e.g., for the optical depth τ within a radiative transfer equation) applied to account for the vegetation influence on the L-band signal. Such parameters are commonly estimated empirically and are validated for specific vegetation types and appropriate phenological characteristics.[13–15] The largely empirically retrieved parameters are very site dependent and vary at low scale to a large degree.[16] The application of vegetation indices retrieved from land surface models [leaf area index (LAI)] or optical remote sensing data (spectral vegetation indices) showed good relationships to optical depth and to account for the vegetation influence on the L-band signal.[17–19] However, using high spatial resolution airborne L-band radiometer data for near surface soil moisture monitoring at the field scale it seems essential to provide information about the heterogeneity that appears even within a "pseudo" homogeneous (one field fruit) vegetation canopy. There is a lack of information based on experimental airborne data to address the effect of vegetation on high spatial resolution brightness temperature observations at L-band within a vegetation canopy previously have been assumed homogeneous (e.g., agricultural fruits).

Therefore, the paper deals with the analyses of experimental airborne high spatial (50×50 m^2) resolution L-band radiometer data according to 1. its vegetation influence mainly represented by LAI and 2. its applicability to estimate near surface soil moisture below crop canopies during the growing season. Information about spatially varying LAI was achieved from high spatial resolution (1.5×1.5 m^2) airborne imaging spectrometer data and LAI field measurements. The retrieved soil moisture values are validated against in-situ measurements of surface soil moisture (6 cm).

2 Study Site and Data

The Helmholtz Association in Germany recently launched an extensive investigation into the long-term effects of climate change at the regional level called Terrestrial Environmental Observatories (TERENO).[20] In the context of TERENO, an airborne soil moisture experiment was performed on May, 26 2008 (DOY 147) over the Harz/Central German Lowland observatory (Fig. 1) to investigate the utility of airborne passive microwave remote sensing of near surface soil moisture at field and regional scales.

The data used within this study is collected over crops, namely winter barley (~27 ha) and winter rye (~37 ha) (Fig. 1). The specific selection of the two test fields was determined by factors such as accessibility and the fact that the sites are within a catchment which is well monitored in terms of water and nutrient fluxes. The topography is gently sloping and the fields consist of loamy sand with ~52% sand and ~11% clay.

2.1 *L-Band Brightness Temperature Data*

L-band passive microwave brightness temperature at two polarizations was observed with the Polarimetric L-Band Multibeam Radiometer (PLMR, ProSensing). For the flights, the PLMR sensor was fitted to a Partenavia PA68 D-GERY aircraft.

PLMR (frequency = 1.413 GHz) utilizes six pushbroom patch array radiometer receivers with viewing angles of ±7 deg (antenna 3 and 4), ±21.5 deg (antenna 2 and 5), and ±38.5 deg (antenna 1 and 6). Horizontal and vertical polarized brightness temperature is measured using a polarization switch.[11] Pre-flight and post-flight calibration, radiometric calibration and final geo-rectification were performed by Airborne Research Australia. Using a reduced antenna beam width, reduced flight speed, and low observation altitude, a ground pixel size of 50 × 50 m^2 was achieved.

To avoid viewing angle dependent effects on the analyses, the horizontal and vertical polarized brightness temperature data was normalized to one viewing angle position like proposed in Ref. 21. For that study the normalization was applied twice; 1. to the two inner (±7 deg) and 2. to the two outer beam positions (±38.5 deg). The reason for that was to evaluate the influence of LAI variations for the ±7 deg and ±38.5 deg viewing angles.

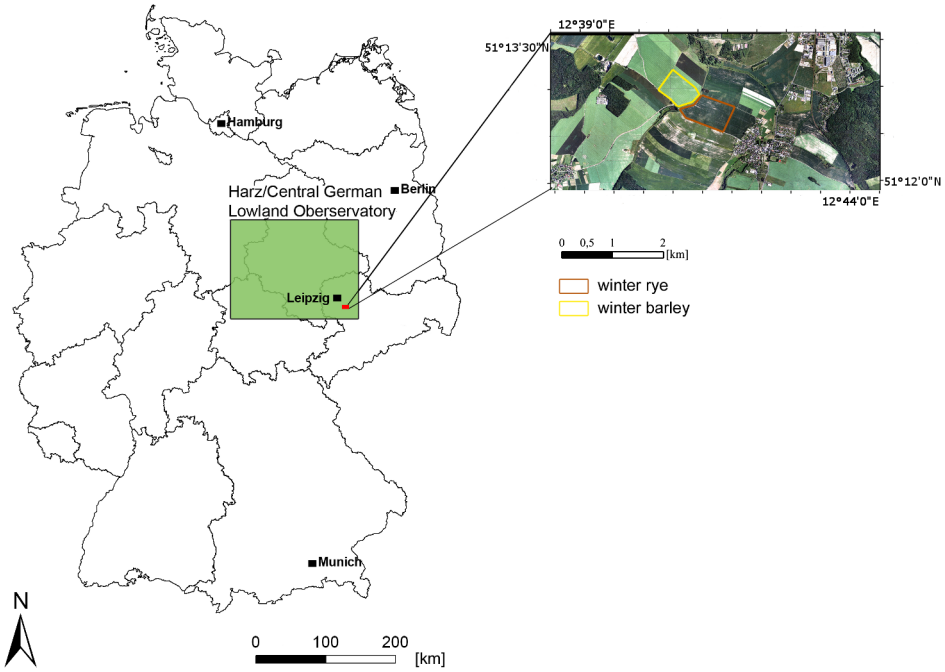

Fig. 1 Location of the winter barley and winter rye site within Germany and within the TERENO Central German Lowland Observatory.

Microwave brightness temperature at L-band is related to the emissivity ε, the physical temperature of the observed surface and to contributions from the atmosphere. Since the atmospheric contribution on L-band brightness temperature data can be neglected because of its atmospheric transmission, emissivity can be calculated by:

$$\varepsilon = \frac{TB}{T}, \tag{1}$$

where T is the physical temperature representing a specific soil or surface layer and measured in Kelvin. Here, the emissivity was calculated for the horizontal brightness temperature data using land surface temperature measurements that were provided by a FLIR S60 thermal imager that recorded simultaneously with PLMR data acquisition. Such temperature data has to be regarded as an integrated signal containing contributions from soil and vegetation. Therefore the emissivity is named $\varepsilon_{\mathrm{surf}}$.

2.2 *Vegetation Data*

At the time of the experiment, the main phenological stage of crops was flowering (main shoot). For winter barley the flowering was more pronounced and fruit sets were mostly visible. To provide spatial distributed information about crop canopy conditions (e.g., LAI) imaging spectrometer data from an [airborne imaging spectro-radiometer (AISA) for application, Specim Ltd.] flight campaign on June, 10 2008 (DOY 162) was applied. Such optical remote sensing data product yields a great information content considering physiological and phenological vegetation parameter retrieval. The time shift of 16 days to the L-band brightness temperature data acquisition (DOY 147) should be regarded critically with respect to changes in plant phenology and its changing influence on the microwave emission. However, the availability of the AISA data set provides scientifically still an interesting and valuable information source for spatial vegetation canopy heterogeneity as presented in the following sections.The available imaging spectrometer data consists of 252 narrow spectral bands collected in the visible and near infrared range of the solar spectrum from 400 to 970 nm. It is provided with a very high pixel ground resolution of 1.5 m $\times$ 1.5 m. Surface reflectance values were achieved by applying the atmospherically correction algorithm MODTRAN using ENVI FLAASH.

On the days of the airborne observations (DOY 147-PLMR sensor and DOY 162—AISA sensor) field LAI data was sampled at geo-rectified sampling point locations. For winter rye 48 and for winter barley 43 ground truth points were sampled. The measurements were determined using a LI-COR, Inc. (Lincoln, Nebraska, USA) LAI-2000 Plant Canopy Analyzer. This compares above- and below-canopy light levels detected in five conical rings, with the view zenith angle ranging from 0 to 75 deg, to infer LAI.[22] On DOY143 (PLMR flight) we found an average LAI of 4.3 for winter barley and 3.6 for winter rye. The height of the winter rye canopy ($\sim$120 cm) was approximately 20 cm higher than the winter barley ($\sim$100) canopy. Canopy height was simply measured by a foot rule. Average vegetation water content for winter barley and winter rye was approximately 2 to 3 kg m^{-2} respective to the apparent phenological stage and confirmed by random field samples.

Linear regression models, field LAI data and narrow band spectral vegetation indices from the AISA data were used to generate high detailed LAI maps with a pixel size of 1.5 $\times$ 1.5 m^2 for the winter barley and winter rye canopy. Therefore, LAI field data achieved on the day of the AISA observation (DOY162) was applied. By field measurements on DOY162 we found an average LAI of 3.9 for winter barley and 3.1 for winter rye. To compute maps of LAI for the two crop types approximately 20 different spectral narrow band vegetation indices were calculated from the 252 collected spectral bands. The tested spectral vegetation indices can roughly be categorized into leaf pigment, vegetation water, and light use efficiency spectral indices. As the linkage between LAI and a spectral vegetation index is not straightforward, crop type specific indices were used to map LAI. For winter barley, the Plant Senescence Reflectance Index PSRI[23] and for winter rye the Modified Triangular Vegetation Index[24] MTVI-2 showed best results ($R^2 = 0.58$ and 0.67, respectively) for estimating LAI under the experiment conditions. The 1.5 $\times$ 1.5 m^2 LAI maps were resampled to 50 $\times$ 50 m^2 pixel LAI maps by

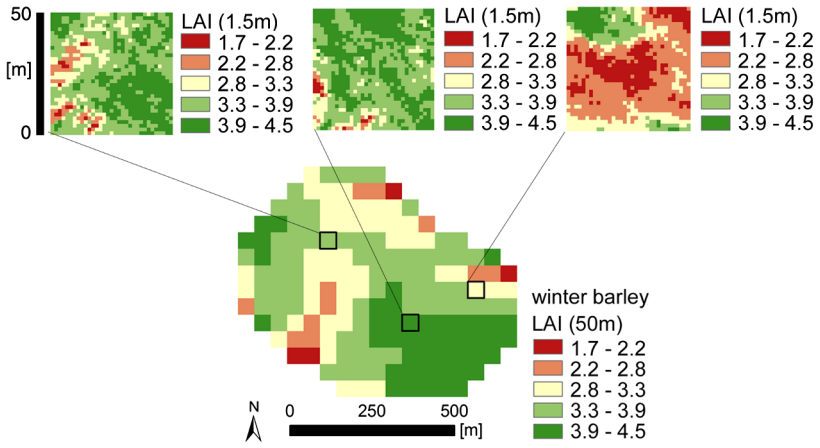

Fig. 2 Visualization of sub-pixel heterogeneity of LAI for winter barley within three examples of 50 $\times$ 50 m^2 pixel representing the cell size of the L-band brightness temperature data.

calculating the pixel average LAI value. Each 50 $\times$ 50 m^2 PLMR pixel includes approximately 1111 LAI pixel of 1.5 m $\times$ 1.5 m^2 cell size. The reason for the spatial averaging was to provide a LAI map with the same pixel size like the brightness temperature observations achieved from the L-band radiometer. Figure 2 visualizes the spatial variability of LAI for 50-m square pixel and appropriate sub-pixel LAI data with 1.5-m square pixel. As can be seen there is a strong variability of LAI even within a homogeneous crop canopy.

2.3 *In- Situ Soil Moisture*

To provide information about inner-field near surface soil moisture heterogeneity in-situ, soil moisture was measured during the airborne data acquisition on DOY 147 (PLMR flight). For winter rye 48 and for winter barley 43 ground truth points were sampled. Because of coverage gaps between the AISA and PLMR data swaths for the combined analyses, a lower number of sampling points (23 for winter barley, 17 for winter rye) is available. Field soil moisture measurements of the 0 to 6 cm layer were performed using mobile ThetaProbe ML2x probes (Delta-T Devices, Ltd., Cambridge, UK). The probe length of 6 cm provided average moisture content of the upper soil layer that is representative for the signal contributing soil layer at L-band.[25]

As can be seen in Fig. 3 the adjacent soil moisture conditions were very dry (<15 Vol.%) during the time of data acquisition. Average soil moisture values of 7.8 Vol.% on the winter barley field and 9.3 Vol.% on the winter rye field were observed at the day of observation.

3 Methods

In order to derive spatially distributed soil moisture data for the test sites, 110 pixel from the winter barley and 152 pixel of the winter rye field from the PLMR data set were used for initially analyzing the influence of pixel average LAI to brightness temperature data at horizontal and vertical polarization. All analyses are performed for the uncorrected data and the brightness temperature normalized to the 7 and 38.5 deg viewing angle positions. Average LAI values were calculated inside each 50-m PLMR pixel. To make the results more clear in terms of interpretation, the brightness temperature data was classified to integer values.

Finally, the correlation between brightness temperature observations and LAI were investigated using linear regression and compared by its coefficient of determination (R^2).

Multi-variate least square regression models (Eq. 2) were applied to estimate near surface soil moisture from a combination of passive microwave data and vegetation related data. The regression coefficients were optimized through the minimization of a least square cost function,

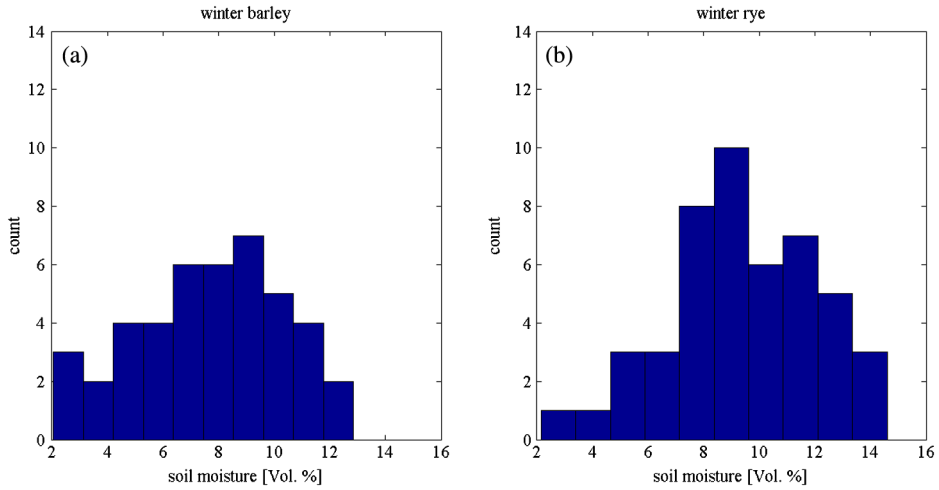

Fig. 3 Histogram of the measured soil moisture of the upper 6 cm soil layer on the winter barley (a) and winter rye (b) test sites during PLMR data acquisition at DOY 147.

$$Y = \beta_0 + \sum_{i=1}^{n} \beta_i \cdot X_i + \varepsilon. \tag{2}$$

As independent variables, microwave surface emissivity ($\varepsilon_{\text{surf}}$) calculated from the horizontally polarizes PLMR brightness temperature and pixel average LAI data achieved at DOY162 were used. In addition to the LAI data, different spectral vegetation indices were added to the set of independent variables. The reason for that was to provide additional information about the heterogeneity of the vegetation canopy and improve the estimation of near surface soil moisture below the vegetation canopy.

Due to coverage gaps between the AISA and PLMR data swaths the regression analysis was performed using 23 sampling points for winter barley and 17 for winter rye. All models were evaluated using the coefficient of determination R^2 and root mean square error (RMSE). Due to the low number of sampling points, we have limited our analysis to a pure calibration exercise demonstrating the influence of high spatial resolution vegetation information on the regression performance. A more extensive calibration/validation analysis using, e.g., split sampling cross validation techniques are planned for the upcoming field campaigns in 2012.

4 Results

4.1 *LAI Influence on High Spatial Resolution L-Band Brightness Temperature*

Regarding the pixel averaged LAI, an obvious relationship between brightness temperature observations and LAI within a crop canopy exists as it is shown in Fig. 4. TB clearly decreases with increasing LAI. As expected from theory, the correlation decreases slightly with decreasing viewing angle for the horizontal polarization. For winter barley, the correlation of the horizontal brightness temperature [Fig. 4(b)] is very strong (e.g., $R^2 = 0.90$ for 7 deg viewing angle). For winter rye the correlation is also obviously visible but appears less linear at those time of data "snap shot." In return, the correlation of the vertical TB [Fig. 4(d)] and LAI for the winter barley data is very weak (e.g., $R^2 = 0.30$ for 7 deg viewing angle) compared to others (e.g., $R^2 = 0.72$ for 7 deg viewing angle and winter rye), which is unexpected because from further studies the vertical polarized data is proposed to be more sensitive to structural vegetation changes. Since with increasing viewing angle the stems become more prominent and increase the attenuation effect of vertical polarization. For winter rye, the correlation with the vertical TB [Fig. 4(c)] data is general stronger than for winter barley, which might be influenced by differences in the canopy height. The winter rye, canopy was approximately 20 cm higher than the winter barley canopy at the day of PLMR data acquisition. Finally, it is obvious that even within a pseudo homogeneous

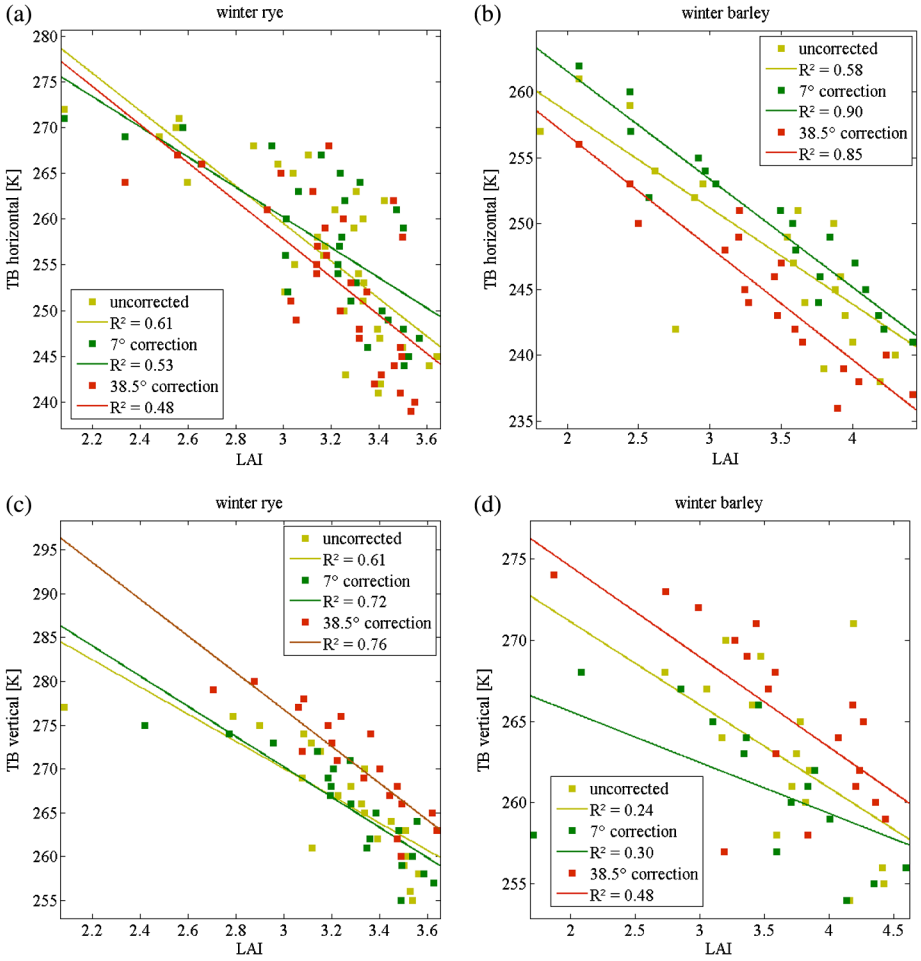

Fig. 4 Three processing stages (uncorrected, 7 deg correction, 38.5 deg correction) of PLMR horizontal [(a) and (b)] and vertical [(c) and (d)] TB plotted against average LAI for winter rye [(a) and (c)] and winter barley [(b) and (d)] data. Linear regression line and coefficient of determination R^2 plotted for each data pair.

vegetation canopy, like here represented by crops, a dependency of within field variations of LAI and corresponding brightness temperature observations exists. Even within very small value ranges of LAI (~2 to 4) the detected microwave signal is clearly influenced. Therefore, it seems useful to provide spatially distributed information about LAI to retrieve spatial soil moisture patterns from passive microwave brightness temperature observations at the field scale.

4.2 *Near Surface Soil Moisture Estimates*

Multi-variate regression models were applied to analyze the sensitivity of microwave emissivity ($\varepsilon_{\text{surf}}$) to compute spatial distributed near surface soil moisture below a crop canopy. The given soil moisture on the day of the experiment was relatively low and varied only within limited range (Fig. 3). Field soil moisture data of the upper 6 cm from the winter rye and winter barley sites were tested crop type specific as dependant variable. As an objective of the study to evaluate the application of a spectral narrow band vegetation index to improve soil moisture predictions, a reduced number of sampling points, namely the AISA-PLMR matching points, were applied for the regression analysis. As can be seen in Fig. 5(a) and 5(b), a correlation between $\varepsilon_{\text{surf}}$ and ground measured soil moisture obviously exists, where $\varepsilon_{\text{surf}}$ slightly increases with decreasing soil moisture. The noise is assumed to represent mainly the vegetation effect on the microwave emissivity. Therefore, we apply the pixel averaged LAI data and tested different

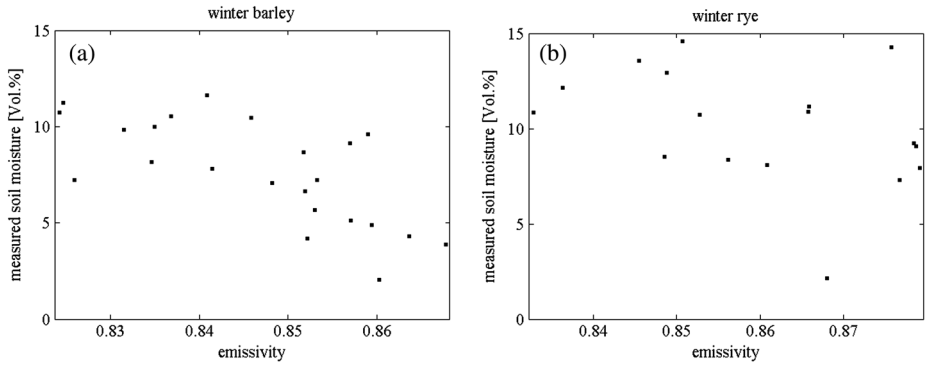

Fig. 5 Observed 0 to 6 cm soil moisture values and plotted against microwave emissivity at L-band for the horizontal polarization at the AISA-PLMR matching points of the winter barley (a) and winter rye field (b).

spectral vegetation indices within the regression analyses to account for the spatially changing noise introduced by the vegetation.

In the following, a stepwise regression analysis is performed using ε_{surf}, pixel averaged LAI, and an additional spectral vegetation index as independent variables. As can be seen in Table 1 for both sites, only very weak model performance is observed when using ε_{surf} as the only explorative variable ($R^2 = 0.48$ for winter barley and 0.15 for winter rye). The weaker soil moisture retrieval results for the winter rye field can very likely be explained by the differences in the vegetation height between the two crop types. The average canopy height of winter rye is 20 cm more than that of winter barley, which clearly results in more biomass per ground unit even when the LAI is lower.

While this procedure (model 1) would relate to a "standard" regression application for soil moisture retrieval using emissivity data only, model performance is significantly improved when considering vegetation data as additional regressors. Adding the pixel averaged LAI (model 2) information, R^2 values increase to 0.82 for winter barley and 0.55 for winter rye. A leaf pigment index, namely the Gitelson Greeness Index[26] calculated from the AISA reflectance, finally introduced the best model results (model 3). The best prediction performance ($R^2 = 0.93$) is achieved for winter barley using the Gitelson Greeness index (GI) and pixel averaged LAI as vegetation proxies and ε_{surf} as independent variables (model 3 for winter barley). Figure 6 provides scatter plots comparing observed soil moisture values versus regression retrieved soil moisture. For winter barley a slight overestimation of soil moisture is observed. Taking into account that

Table 1 Coefficient of determination (R^2), root mean square error (RMSE), and equation of multivariate regression models for estimating near surface soil moisture by different sets of independent variables (ε_{surf}- surface emissivity, LAI—leaf area index, and GI—Gitelson Greeness Index) from the winter barley and winter rye test site.

		Winter barley			Winter rye		
model	Independent variable set	R^2	RMSE [Vol.%]	equation	R^2	RMSE [Vol.%]	Equation
model 1	ε_{surf}	0.48	2.0	$y = -143.3\varepsilon_{surf} + 129$	0.15	2.94	$y = -78.5101\varepsilon_{surf} + 77.6334$
model 2	LAI,ε_{surf}	0.82	1.43	$y = -99.4553\varepsilon_{surf} + 3.1067\text{LAI} + 78.4038$	0.55	4.85	$y = -36.7348\varepsilon_{surf} + 5.1578\text{LAI} + 23.5133$
model 3	LAI, GI,ε_{surf}	0.93	0.58	$y = -93.4586\varepsilon_{surf} + 1.7451\text{LAI} + 2.1741\text{GI} + 77.2960$	0.73	3.14	$y = -1.0092\varepsilon_{surf} + 4.9746\text{LAI} + 2.2342\text{GI} - 11.9129$

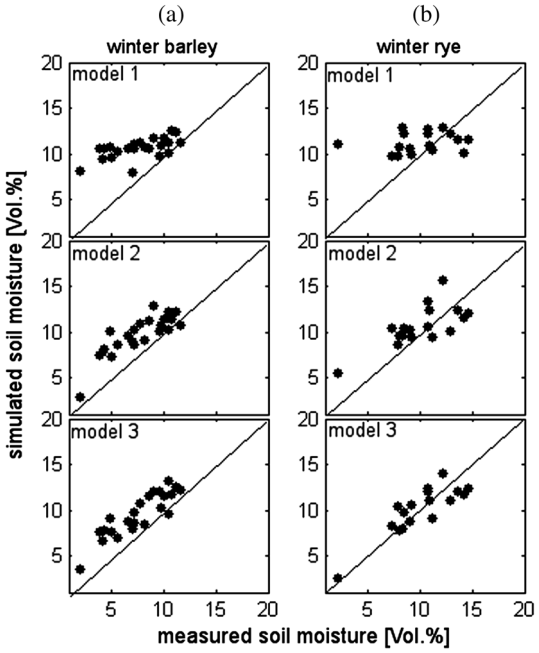

Fig. 6 Scatter plots of observed soil moisture versus regression derived soil moisture for winter barley (a) and winter rye (b) at DOY 147 of the year 2008.

the average observed soil moisture on the winter barley site is slightly lower than on winter rye, this overestimation might be explained by a limitation in detecting soil moisture variations for very dry soils and below a dense green vegetation canopy. Maps of the final near surface soil moisture computed using model 3 are given within Fig. 7.

It seems the Gitelson Greeness Index is able to provide additional information about vegetation heterogeneity influencing the observed brightness temperature and surface emissivity, respectively. The main difference of the Gitelson Greeness Index compared to the most other tested is that it does not use a spectral band of the red region of the electromagnetic spectrum. Therefore it is proposed to be less sensitive for saturation effects introduced from LAI and green leaf biomass.[26] Within this experiment the information introduced by the Gitelson Index supports very well the LAI information to account for the vegetation effect on the land surface emissivity at L-band.

Currently the results of the study can barely be compared with other studies using L-band brightness temperature since the observation characteristics (e.g., observation angle, frequency, polarization) and the type of vegetation cover (e.g., crop type, phenological stage) are very experiment specific. To remotely estimate surface soil moisture from microwave data at field scale synthetic aperture radar (SAR) data was mostly applied so far, which is motivated by its higher spatial resolution. The spatial scale of observation and the finally achieved pixel size is a key parameter that needs to be similar for comparison issues.

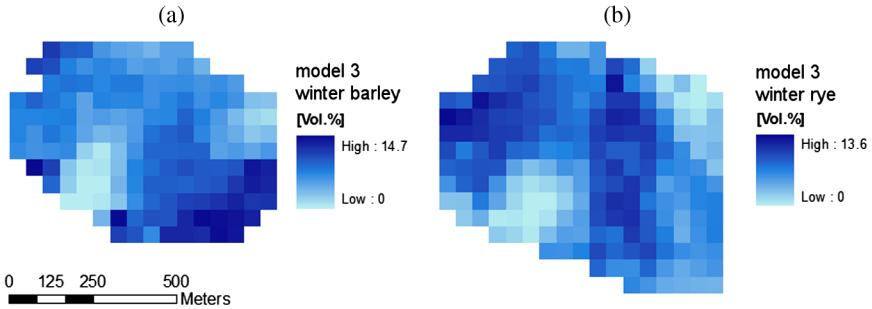

Fig. 7 Maps of near surface soil moisture (pixel size 50 $\times$ 50 m^2) achieved using model 3 for a winter barley (a) and a winter rye (b) site at DOY 147 of the year 2008.

However, in Ref. 27 the retrieval of surface soil moisture from L-band brightness temperature is studied using experimental data collected by a field radiometer over a 72×16 m^2 bare soil plot. Time domain reflectometry (TDR) measurements were used as reference. Comparing averaged radiometer results and TDR measurements a $R^2 = 0.67$ was achieved with 0.4 as slope value for the regression line. In Ref. 28 a support vector regression technique is applied to estimate the dielectric constant from bare soils. The coefficient of determination of estimated versus measured dielectric constant values was $R^2 = 0.75$ for the best case. Considering the results of the above mentioned studies from bare soils the results achieved within this study ($R^2 = 0.93$ for winter barley, $R^2 = 0.73$ for winter rye) motivate the application of L-band radiometer data for soil moisture studies over vegetated soils (e.g., agricultural sites) to detect soil moisture variabilities at field scale level. In Ref. 29 semi-empirical regressions to assess the soil moisture retrieval from L-band brightness temperature over natural grass are applied. They derived the regressions analytically from the L-Band Emission of the Biosphere model (L-MEB) and evaluated its performance under different rainfall interception conditions. Regressions considering different configurations of viewing angles and polarizations were considered and $R^2 = 0.73$ were achieved for the best case.

As the achieved pixel size from passive microwave data at L-band is generally low (several hundred meters up to many kilometres) from satellite and airborne observations, the description of land surface heterogeneity has a different level of detail compared to high spatial resolution airborne observations. For example, in Ref. 30 a global regression study is performed to retrieve soil moisture from L-band radiometer data with a spatial resolution of half a degree. Hereby, a 1-km land cover map was applied to account for land surface heterogeneity. However, the application of spectral vegetation indices [mainly normalized difference vegetation index (NDVI)] is well known in microwave soil moisture studies. For instance, spectral vegetation indices derived from satellite data are used to empirically estimate area wide vegetation water content or LAI that are in turn applied to compute optical depth values required as input for soil moisture retrieval using radiative transfer models.[16]

5 Summary and Conclusion

Low-frequency passive microwave remote sensing at L-band (~1.4 GHz) has been found to be the most promising remote sensing method for soil moisture monitoring due to the direct link between microwave radiation and dielectric properties, its deeper penetration into vegetation, its all-weather capabilities, and its negligible atmospheric attenuation. The soil moisture sensitivity of L-band brightness temperature changes spatially with soil, vegetation, and terrain characteristics. The contribution of surface soil moisture on observed brightness temperature data at L-band is highly spatial variable as it is strongly influenced from the vegetation cover of the soil that is presented in this study for crop canopies. Attenuation and scattering processes within a vegetation canopy are strongly influenced by specific geometrical (e.g., LAI, canopy height) and biophysical (e.g., vegetation water content) vegetation canopy characteristics. In order to estimate soil moisture below a vegetation canopy it is essential to provide spatial distributed information about vegetation characteristics.

The results presented in Sec. 4.1 show an obvious ($0.23 < R^2 < 0.90$) relationship between the microwave brightness temperature observations and LAI variations within a vegetation canopy that is usually assumed being homogeneous.

The empirical analysis given in Sec. 4.2 has shown a strong field fruit dependent sensitivity of the microwave emissivity for estimating near surface soil moisture. L-band sampling of surface soil moisture depends mainly on the characterization of the vegetation, as this study shows on a field scale level for a vegetation canopy that is in microwave soil moisture studies generally treated homogeneous. Even vegetation canopy variations within one field fruit strongly affect the soil moisture retrieval. A lack of information about the spatially varying vegetation canopy (e.g., LAI) reduces the retrieval opportunity of any soil moisture algorithm. In this study, the weaker performance for the winter rye site is explained by the difference of the vegetation canopy height. Due to the higher plants the emitted microwave radiation coming from the soil is much more attenuated.

For application oriented use of L-band microwave data it is generally not clear how strong the signals soil moisture sensitivity changes from pixel to pixel regarding spatial variation of vegetation characteristics. The final conclusions are summarized as follows:

- The general spatial pattern of vegetation influence on the microwave signal seems very well reflected by the applied LAI data and the Gitelson Greeness Index (GI). In microwave soil moisture studies GI might also be treated as a proxy for fresh green leaf biomass.
- The results demonstrate that reasonable estimates of surface soil moisture on field scale are possible using multi-variate regression.
- As the vegetation canopy characteristics (e.g., canopy height and LAI) may strongly change during the growing season and within the site it is recommended to provide spatially distributed information about the actual vegetation canopy. Point measurements of LAI may also strongly improve the soil moisture retrieval accuracy but a site wide global parameterization of LAI will result in a loss of information about the actual soil moisture pattern.
- Remote detection of surface soil moisture by the PLMR passive microwave sensors in combination with imaging spectrometer data has the advantage of providing spatial integrated information even without in-situ vegetation data as required for monitoring issues.

For instance, with the launch of the German hyperspectral satellite Environmental Mapping and Analyses Program (EnMAP) scheduled for 2014, valuable spatial distributed vegetation information will be available to support soil moisture retrieval algorithms using airborne and satellite L-band microwave data from the plot up to the catchment scale.

It has to be noted that given the one-day availability of the PLMR sensor during the field campaigns, it has been impossible to analyze the method presented here to a wider range of soil moisture conditions. It is planned for further campaigns to extend this analyses to a larger variety of climate weather conditions and also to investigate the applicability of the PLMR sensor for other crop types and different phenological stages.

While the spatial resolution of satellite borne passive L-band radiometer data is still too coarse for agricultural applications, airborne L-band radiometer sensor data have shown here to be a valuable information source for agricultural management or small catchment monitoring. Their almost weather independent application make them a valuable method for monitoring. Optical broad band (spectral) remote sensing data products from satellites are available with regular temporal coverage and a fine spatial pixel size (<30 m) and may be included in the analyses in case no airborne optical data product can be achieved parallel to L-band radiometer data.

Ongoing research will investigate the potential of spectral vegetation indices achieved from optical broad and narrow band remote sensing data products to condition the optimization of the parameterization of physically based radiative transfer models to derive near surface soil moisture from airborne high spatial resolution L-band radiometer data.

Acknowledgments

The research was funded and supported by TERENO (Terrestrial Environmental Observatories), which is a joint collaboration program of several Helmholtz Research Centers in Germany. Furthermore, the work was supported by a scholarship of the German Federal Foundation for Environment (DBU) and additionally funded by the Helmholtz-Centre for Environmental Research, UFZ, and the Ministry for Science, Research and Arts Baden-Württemberg.

References

1. R. B. Grayson and A. W. Western, "Towards areal estimation of soil water content from point measurements: time and space stability of mean response," *J. Hydrol.* **207**(1–2), 68–82 (1998), http://dx.doi.org/10.1016/S0022-1694(98)00096-1.
2. K. Schulz et al., "Importance of spatial structures in advancing hydrological sciences," *Water Resour. Res.* **42**(3), 2–5 (2006), http://dx.doi.org/10.1029/2005WR004301.

3. E. Zehe et al., "Patterns of predictability in hydrological threshold systems," *Water Resour. Res.* **43**(7) (2007), http://dx.doi.org/10.1029/2006WR005589.
4. H. Vereecken et al., "On the value of soil moisture measurements in vadose zone hydrology: a review," *Water Resour. Res.* **44** (2008), http://dx.doi.org/10.1029/2008WR006829.
5. R. Cardell-Oliver et al., "A reactive soil moisture sensor network: design and field evaluation," *Int. J. Distrib. Sens. N.* **1**(2), 149–162 (2005), http://dx.doi.org/10.1080/15501320590966422.
6. D. A. Robinson et al., "Soil moisture measurement for ecological and hydrological watershed-scale observatories: a review," *Vadose Zone J.* **7**(1), 358–389 (2008), http://dx.doi.org/10.2136/vzj2007.0143.
7. Y. H. Kerr, "Soil moisture from space: where are we?," *Hydrogeol. J.* **15**(1), 117–120 (2007), http://dx.doi.org/10.1007/s10040-006-0095-3.
8. W. Wagner et al., "Operational readiness of microwave remote sensing of soil moisture for hydrologic applications," *Nord. Hydrol.* **38**(1), 1–20 (2007), http://dx.doi.org/10.2166/nh.2007.029.
9. K. Blyth, "The use of microwave remote sensing to improve spatial parameterization of hydrological models," *J. Hydrol.* **152**(1–4), 103–129 (1993), http://dx.doi.org/10.1016/0022-1694(93)90142-V.
10. S. Delwart et al., "SMOS validation and the COSMOS campaigns," *IEEE T. Geosci. Remote* **46**(3), 695–704 (2008), http://dx.doi.org/10.1109/TGRS.2007.914811.
11. R. Panciera et al., "The NAFE'05/CoSMOS data set: toward SMOS soil moisture retrieval, downscaling, and assimilation," *IEEE T. Geosci. Remote* **46**(3), 736–745 (2008), http://dx.doi.org/10.1109/TGRS.2007.915403.
12. T. J. Jackson, T. J. Schmugge, and P. O'Neill, "Passive microwave remote sensing of soil moisture from an aircraft platform," *Remote Sens. Environ.* **14**(1–3), 135–150 (1984), http://dx.doi.org/10.1016/0034-4257(84)90011-7.
13. T. J. Jackson, "Measuring surface soil-moisture using passive microwave remote sensing," *Hydrol. Process.* **7**(2), 139–152 (1993), http://dx.doi.org/10.1002/(ISSN)1099-1085.
14. T. J. Jackson and T. J. Schmugge, "Vegetation effects on the microwave emission of soils," *Remote Sens. Environ.* **36**(3), 203–212 (1991), http://dx.doi.org/10.1016/0034-4257(91)90057-D.
15. E. G. Njoku and D. Entekhabi, "Passive microwave remote sensing of soil moisture," *J. Hydrol.* **184**(1–2), 101–129 (1996), http://dx.doi.org/10.1016/0022-1694(95)02970-2.
16. J. P. Wigneron et al., "L-band microwave emission of the biosphere (L-MEB) Model: description and calibration against experimental data sets over crop fields," *Remote Sens. Environ.* **107**(4), 639–655 (2007), http://dx.doi.org/10.1016/j.rse.2006.10.014.
17. T. J. Jackson et al., "Vegetation water content mapping using Landsat data derived normalized difference water index for corn and soybeans," *Remote Sens. Environ.* **92**(4), 475–482 (2004), http://dx.doi.org/10.1016/j.rse.2003.10.021.
18. T. J. Jackson et al., "Soil moisture mapping at regional scales using microwave radiometry: the Southern Great Plains hydrology experiment," *IEEE T. Geosci. Remote* **37**(5), 2136–2151 (1999), http://dx.doi.org/10.1109/36.789610.
19. K. Saleh et al., "Impact of rain interception by vegetation and mulch on the L-band emission of natural grass," *Remote Sens. Environ.* **101**(1), 127–139 (2006), http://dx.doi.org/10.1016/j.rse.2005.12.004.
20. S. Zacharias et al., "A network of terrestrial environmental observatories in Germany," *Vadose Zone J.* **10**(3), 955–973 (2011), http://dx.doi.org/10.2136/vzj2010.0139.
21. T. J. Jackson et al., "Large area mapping of soil moisture using the ESTAR passive microwave radiometer in Washita '92," *Remote Sens. Environ.* **54**(1), 27–37 (1995), http://dx.doi.org/10.1016/0034-4257(95)00084-E.
22. J. M. Welles and J. M. Norman, "Instrument for indirect measurement of canopy architecture," *Agron. J.* **83**(5), 818–825 (1991), http://dx.doi.org/10.2134/agronj1991.00021962008300050009x.
23. M. N. Merzlyak et al., "Non-destructive optical detection of pigment changes during leaf senescence and fruit ripening," *Physiol. Plant.* **106**(1), 135–141 (1999), http://dx.doi.org/10.1034/j.1399-3054.1999.106119.x.

24. D. Haboudane et al., "Hyperspectral vegetation indices and novel algorithms for predicting green LAI of crop canopies: modeling and validation in the context of precision agriculture," *Remote Sens. Environ.* **90**(3), 337–352 (2004), http://dx.doi.org/10.1016/j.rse.2003.12.013.
25. T. J. Schmugge, "Remote sensing of soil-moisture—recent advances," *IEEE T. Geosci. Remote* **GE-21**(3), 336–344 (1983), http://dx.doi.org/10.1109/TGRS.1983.350563.
26. A. A. Gitelson et al., "Remote estimation of leaf area index and green leaf biomass in maize canopies," *Geophys. Res. Lett.* **30**(5), 1248–1251 (2003), http://dx.doi.org/10.1029/2002GL016450.
27. F. Jonard et al., "Mapping field-scale soil moisture with L-band radiometer and ground-penetrating radar over bare soil," *IEEE T. Geosci. Remote* **49**(8), 2863–2875 (2011), http://dx.doi.org/10.1109/TGRS.2011.2114890.
28. L. Pasolli, C. Notarnicola, and L. Bruzzone, "Estimating soil moisture with the support vector regression technique," *IEEE T. Geosci. Remote Sens. Lett.* **8**(6), 1080–1084 (2011), http://dx.doi.org/10.1109/LGRS.2011.2156759.
29. K. Saleh et al., "Semi-empirical regressions at L-band applied to surface soil moisture retrievals over grass," *Remote Sens. Environ.* **101**(3), 127–139 (2006), http://dx.doi.org/10.1016/j.rse.2006.01.008.
30. T. Pellarin, J. C. Calvet, and J. P. Wigneron, "Surface soil moisture retrieval from L-band radiometry: a global regression study," *IEEE T. Geosci. Remote* **41**(9), 2037–2051 (2003), http://dx.doi.org/10.1109/TGRS.2003.813492.

Biographies and photographs of the authors are not available.